

# Electrostatic Charges Regulate Chemiluminescence by Electron Transfer at the Liquid–Solid Interface

Jinyang Zhang,<sup>||</sup> Shiquan Lin,<sup>||</sup> and Zhong Lin Wang\*<sup>||</sup>



Cite This: <https://doi.org/10.1021/acs.jpcb.1c09402>



Read Online

ACCESS |



Metrics & More

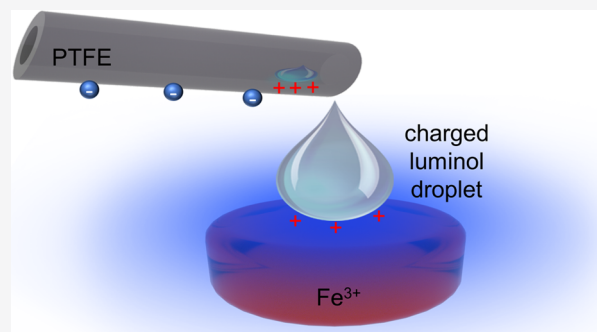


Article Recommendations



Supporting Information

**ABSTRACT:** The role of the electrostatic environment in chemical reactions has long been an important research field, but most studies have focused on the influence of external electric fields on chemical processes, while the effect from the intrinsic electrostatic charges on the solution itself has been ignored. How an electrostatic field generated by contact electrification affects the solvent environment in a chemical reaction and then the chemical reactivity is still ambiguous. Here, based on the inspiration of the droplet triboelectric nano-generator, electrostatic interactions between a statically charged luminol droplet and the surrounding directional electrostatic field were analyzed, and we demonstrate a relationship between the sign of the luminol sample (negatively or positively charged) and its effect on the reaction reactivity. Our results show that the enhanced reaction activity and the enhanced chemiluminescence (CL) only occurred when the luminol droplet yields positive charges, while a negatively charged luminol, on the contrary, tends to inhibit the CL, which brings direct evidence of the charge carriers of triboelectricity being electrons at the liquid–solid interface. This work provides a strategy for electrostatically regulating CL by simply statically charging a reaction solution with a dielectric solid and also carries a cautionary message on what to consider when preparing a sample for a chemical reaction.



group developed a self-powered droplet triboelectric nano-generator with spatially arranged electrodes as a probe for measuring the charge transfer (CT) between liquid and solid interfaces and showed that the electron transfer is the dominant CT species in the case of liquid/solid contact.<sup>20</sup> This inevitably raises a challenge about the reproducibility of the chemical reaction in the liquid solution as chemical reactivity is governed by the movement and transfer of electrons, and electron transfer is most likely to occur at the interface between the reaction solution and the surrounding environment or the container,<sup>21,22</sup> such as air, beaker and pipette, when preparing the reaction solution. Most importantly, it provides a chance to harness electrostatic field to control chemical reactivity in bulk chemical reaction solution. Recently, some research groups have focused on the chemical reactivity governed by the electrostatic charges, they showed the relationship between a plastic sample's net negative charge and the amount of solution metal ions discharged to metallic particles with a coefficient of

## 1. INTRODUCTION

The electrostatic field in chemical reactions, which enables control over wide-ranging aspects of chemical reactivity and structure, has long been an important research field and has attracted many scientists to devote on it.<sup>1–4</sup> While most of the research to date have been computational,<sup>5</sup> the landmark experiment was conducted by Aragonés et al. in 2016.<sup>6</sup> In this experiment, the authors used scanning tunnelling microscopy to both deliver the electric field and to measure its effect on the single-molecule reaction rate (bond-forming and bond-breaking). This experiment is important and provides the first experimental demonstration of a directional electric field affecting reaction kinetics. However, to scale up these experiments to widely applicable techniques to harness electrostatic field in the bulk solution of chemical reaction is still difficult. Therefore, alternative approaches for harnessing electrostatic fields to control chemical reactivity are required.

Fortunately, over the last 5–10 years, a growing number of research groups have noticed one type of electrostatic field, which can be simply generated by contact electrification without any applied voltage or additives.<sup>7–10</sup> Static charges develop on the surface of electrically insulating materials that are first brought in contact with and then macroscopically separated from another solid.<sup>11,12</sup> Recent studies show that this phenomenon is not limited to the solid/solid interface but also occurred at the liquid/solid or liquid/liquid interface.<sup>13–19</sup> Based on the contact charging at the liquid/solid interface, our

group developed a self-powered droplet triboelectric nano-generator with spatially arranged electrodes as a probe for measuring the charge transfer (CT) between liquid and solid interfaces and showed that the electron transfer is the dominant CT species in the case of liquid/solid contact.<sup>20</sup> This inevitably raises a challenge about the reproducibility of the chemical reaction in the liquid solution as chemical reactivity is governed by the movement and transfer of electrons, and electron transfer is most likely to occur at the interface between the reaction solution and the surrounding environment or the container,<sup>21,22</sup> such as air, beaker and pipette, when preparing the reaction solution. Most importantly, it provides a chance to harness electrostatic field to control chemical reactivity in bulk chemical reaction solution. Recently, some research groups have focused on the chemical reactivity governed by the electrostatic charges, they showed the relationship between a plastic sample's net negative charge and the amount of solution metal ions discharged to metallic particles with a coefficient of

**Received:** October 29, 2021

**Revised:** February 11, 2022

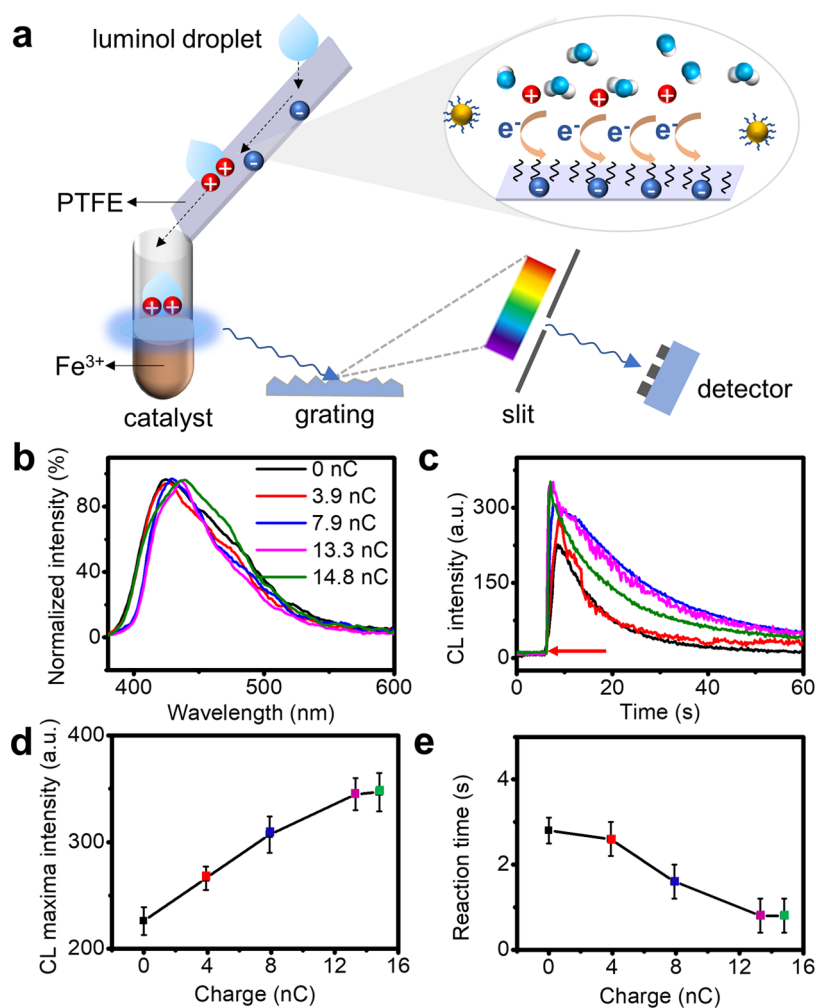


**Figure 1.** Positively charged luminol droplet promotes the CL reaction. (a) Experimental setup. When a drop of luminol solution flows through the PTFE surface, the electron transfer between luminol and solid occurred, and then the statically charged luminol was dropped into the cuvette containing the catalyst, leading to light blue emission. (b) Normalized emission spectra recorded for the  $\text{Fe}^{3+}$  catalysis statically charged luminol droplet (8 mM luminol, 0.1 M sodium hydroxide, and 0.1 M hydrogen peroxide) of net charge 0,  $3.9 \pm 0.4$ ,  $7.9 \pm 0.5$ ,  $13.3 \pm 0.8$ , and  $14.8 \pm 1.3$  nC. (c) Time-resolved emission intensity data (425 nm). The solid red arrow indicates when the luminol droplet (50  $\mu\text{L}$ ) is dropped into the quartz vessel containing the catalyst  $\text{Fe}^{3+}$ . (d) CL maxima intensity (425 nm) measured as the function of charge (Faraday pail measurements) for luminol droplet flowing through the PTFE surface. (e) Reaction time measured as the function of charge [note that the reaction time here refers to the time from when the luminol droplet reacts with the catalyst to the maximum CL intensity (425 nm)].

proportionality linked to its electron affinity.<sup>9</sup> However, the evidence of electrostatic field generated by contact electrification effects on the chemical reactivity and reaction rate is still ambiguous and needs to be understood.

The purpose of this work is to provide a strategy for electrostatic regulation of chemiluminescence (CL) by simply statically charging a reaction solution with a dielectric solid. We have quantified the light intensity and the reaction rate of CL on the potassium ferricyanide catalysis electrostatically charged luminol droplet that was charged to either net positive or net negative Coulomb values. The positive charged luminol droplet promotes the luminescence reaction for both speeding up the reaction and enhancing the luminescence, while the negatively charged luminol, on the contrary, inhibits the reaction. We postulated therefore the possible influence of the electric double layer and electron transfer on the catalytic reaction. Moreover, the electrostatic environment sensed by the excited state of a light-emitting molecule affecting the energy of its radiative decay should be a reason for the unstable position of the emission peak. Further, this is recent and

compelling evidence from a chemical perspective, indicating that the charge-carrying species, accounting for statics in the liquid/solid interface, are electrons.

## 2. EXPERIMENTAL DETAILS

**2.1. Chemicals and Materials.** Redistilled solvents and Milli-Q water ( $>18 \text{ M}\Omega \text{ cm}$ ) were used for substrate cleaning and to prepare solutions. Tubes of polytetrafluoroethylene (PTFE,  $d = 1 \text{ cm}$ ), nylon ( $d = 1 \text{ cm}$ ), polyvinyl chloride (PVC,  $d = 1 \text{ cm}$ ), and fluorinated ethylene propylene (FEP,  $d = 1 \text{ cm}$ ) were used for contact with the luminol droplets. Luminol (3-aminophthalhydrazide, 97%), sodium hydroxide (99.99%), potassium ferricyanide (99%), hydrogen peroxide (aqueous, 30% w/w), potassium permanganate (99%), and copper sulfate (99%) were purchased from Sigma.

**2.2. Charge Measurements.** All plastic tubes with different lengths were extensively washed with ethanol prior to each experiment to remove static charges, and then the luminol droplet was slid through the tubes and statically charged against the tubes' surface. When specified, the

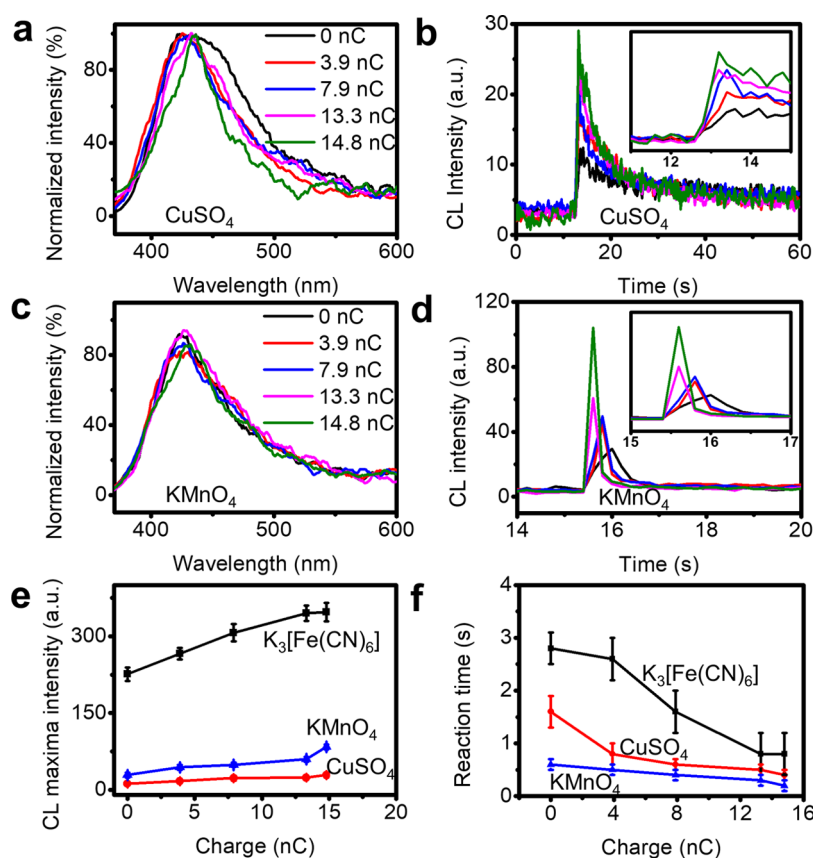


**Figure 2.** Role of electrostatic charge on the catalytic performance of CL reaction with various catalysts. (a) Normalized emission spectra recorded for  $\text{CuSO}_4$  catalysis statically charged luminol droplet (8 mM luminol, 0.1 M sodium hydroxide, and 0.1 M hydrogen peroxide). (b) Time-resolved emission intensity data (425 nm) when the catalyst is  $\text{CuSO}_4$  solution. (c) Normalized emission spectra recorded for the  $\text{KMnO}_4$  catalysis statically charged luminol droplet (8 mM luminol, 0.1 M sodium hydroxide, and 0.1 M hydrogen peroxide). (d) Time-resolved emission intensity data (425 nm) when the catalyst is  $\text{KMnO}_4$  solution. (e) CL maxima intensity (425 nm) measured as the function of charge (Faraday pail measurements) for the luminol droplet flowing through the PTFE surface and then dropped to different catalysts. (f) Reaction time measured as the function of charge [note that the reaction time here refers to the time from when the luminol droplet reacts with the different catalysts to the maximum CL intensity (425 nm)].

magnitude of the sample net charge was varied by changing the length of the plastic tube. Sample charges were measured by a nanocoulomb meter (model 284, Monroe Electronics, USA) operating on the  $10^{-9}$  C scale. The amount of charge on the luminol droplet is the mean of 10 independent experiments (Faraday measurements).

**2.3. Luminescence Experiments.** The luminol droplet contained 8 mM luminol, 0.1 M sodium hydroxide, and 0.1 M hydrogen peroxide. After the luminol droplet slid through the plastic tube, it was dropped to a cuvette containing 100  $\mu\text{L}$  of potassium ferricyanide solution (3 mM) (Figure 1a, and a blue light was obtained. The cuvette containing the catalyst was placed inside a FLS980-S2S2-STM fluorescence spectrophotometer.

### 3. RESULTS AND DISCUSSION

Figure 1a shows the experimental design, where a luminol droplet (50  $\mu\text{L}$  per drop), containing 8 mM luminol, 0.1 M sodium hydroxide, and 0.1 M hydrogen peroxide was first released from a grounded stainless-steel needle (3 mm diameter), to remove the static charges, by a syringe pump at a fixed height (1 cm) above the dielectric polymer surface with a tilted angle. The optical photograph of the light emission of the system is seen in Supporting Information Figure S1. The net charge of the luminol droplet sample was

assessed by means of a Faraday pail measurement. The luminol droplet was made to rapidly flow through a dielectric solid surface, for example, a PTFE tube. At this stage, the electron transfer occurs at the liquid/solid interface,<sup>20,23,24</sup> leading to the positively charged luminol droplet as well as the negatively charged PTFE. The process of contact electrification between the luminol droplet and PTFE causes the reaction solution to generate the electric charge and thus probably an electric field. After the statically charged luminol was dropped into the cuvette containing the catalyst, such as  $\text{Fe}^{3+}$ , blue light emissions could be observed and were captured by a fluorescence spectrophotometer. Figure 1b shows the emission spectra recorded immediately after completing the addition of a luminol droplet with different net charges to  $\text{Fe}^{3+}$  solution. The magnitude of the net charge was varied by changing the length of the PTFE tube. From Figure 1b, it can be seen that the band was centered at  $425 \pm 2$  nm when there is no static charge (no contact with PTFE and 0 nC measured by Faraday pail) on the luminol droplet. The 425 nm emission has been previously suggested to originate from the decay of excited luminol-derived 3-aminophthalate (3-APA\*) in bulk water.<sup>25</sup> This form is stabilized in water through a H-bonding network involving the neighboring oxygen of the carboxylic group. However, when the luminol droplet starts to be statically charged, that is, after it contacts with the PTFE, the range of

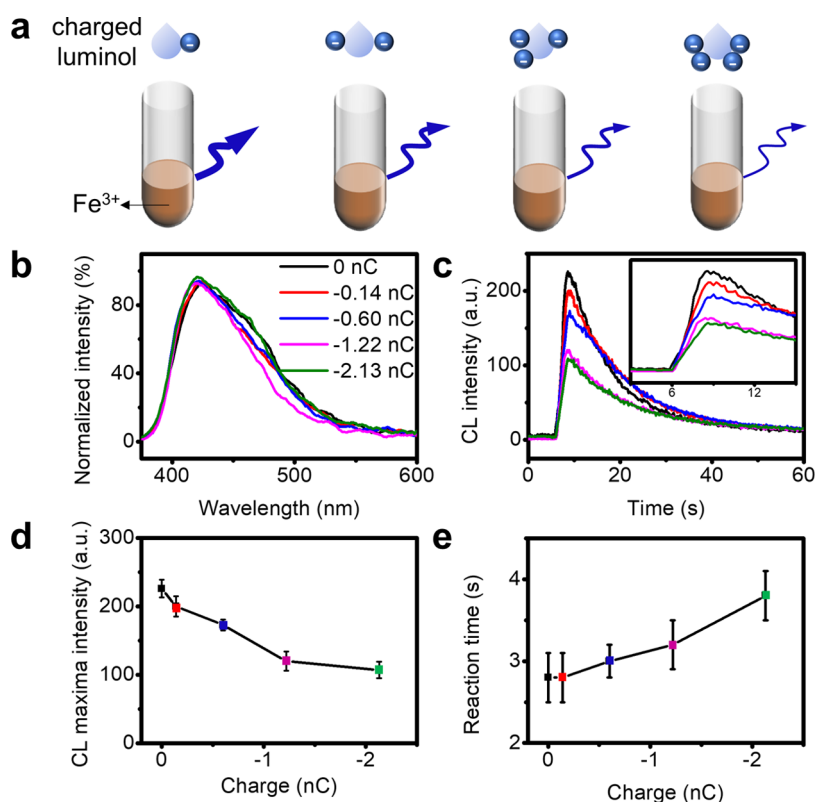


**Figure 3.** Negatively charged luminol droplet inhibits the CL reaction. (a) More negative charges on the luminol droplet leads to weaker CL emission. The density of the sample's net charges was varied by changing the length of the nylon tube. (b) Normalized emission spectra recorded for the  $\text{Fe}^{3+}$  catalysis negatively charged luminol droplet (8 mM luminol, 0.1 M sodium hydroxide, and 0.1 M hydrogen peroxide) of net charge 0,  $-0.14 \pm 0.05$ ,  $-0.6 \pm 0.08$ ,  $-1.22 \pm 0.2$ , and  $-2.13 \pm 0.4$  nC. (c) Time-resolved emission intensity data (425 nm) measured as the function of charge (Faraday pail measurements) for the luminol droplet flowing through the nylon surface. (d) CL maxima intensity (425 nm) measured as the function of charge. (e) Reaction time measured as the function of charge.

the band center is expanded (420–439 nm). This seems like a single emitter but sensing different electrostatic environments. The luminol excited state is supposed to have a CT character, it is therefore most likely that the change in energy is due to unstable/stabilization of the CT by the electric field from the statically charged reaction solution (charged luminol droplet).<sup>26</sup>

To further explore the electrostatic effect on the luminescence experiment, the time-resolved emission intensity data (425 nm) of different net charges on luminol were recorded. The solid red arrow in Figure 1c indicates when the luminol droplet is dropped into the quartz vessel containing the catalyst  $\text{Fe}^{3+}$ . We note that the maxima light intensity scales with the net charging magnitude of the luminol droplet: the higher the static charges of the luminol droplet, the stronger the CL maxima intensity (Figure 1c,d). For the charged luminol– $\text{Fe}^{3+}$  system, stronger CL emission was observed with the addition of the charged luminol droplet into the  $\text{Fe}^{3+}$  solution as compared to the weaker CL emission in the absence of a static charge on the luminol droplet (Figure 1c), indicating the excellent catalytic performance of the statically charged luminol– $\text{Fe}^{3+}$  system. Meanwhile, the catalytic activity of the charged luminol– $\text{Fe}^{3+}$  system increased with the increase in charge on the luminol droplet (Figure 1d), which proves the role of electrostatic charge on the catalytic performance of the CL reaction. Moreover, the time to reach the CL maxima intensity (reaction time) of the luminol samples of different initial charges has also been studied. Although the CL maximum intensity increases with the

increase in the amount of static charge on the luminol droplet, the time to reach the CL maximum intensity decreases with the increase in the amount of static charges. What becomes apparent for the first time is that the static charges generated by the liquid/solid contact on the liquid droplet affects the reaction rate of the CL reaction. This phenomenon was not only observed for the luminol/PTFE system but was also observed for other dielectric materials, such as FEP and PVC (Supporting Information, Figure S2). FEP and PTFE have a stronger affinity to electrons compared with PVC;<sup>27</sup> therefore, higher electron-transfer abilities were observed for FEP and PTFE, and stronger CL emissions were obtained. This supports the electron transfer at the liquid–solid interface.

The relationship between the CL intensity and the concentration of potassium ferricyanide has already been widely reported: the CL intensity sharply increases with an increase in the concentration of potassium ferricyanide.<sup>28,29</sup> This is consistent with our result in Figure S3a. Meanwhile, we have also studied the relationship between the reaction rate and the concentration of potassium ferricyanide in Figure S3b. The result shows that the reaction rate increases with an increase in the concentration of potassium ferricyanide. We speculate that the effect of potassium ferricyanide on the CL intensity and reaction rate is mainly from the effect of  $\text{Fe}^{3+}$  on the decomposition reaction of hydrogen peroxide and thus the generation of  $\text{O}_2$  ( $\text{Fe}^{3+} + \text{HO}_2^- \rightarrow \text{FeHO}_2^{2+}$ ,  $\text{FeHO}_2^{2+} \rightarrow \text{OH}^- + \text{FeO}^{3+}$ ,  $\text{FeO}^{3+} + \text{HO}_2^- \rightarrow \text{OH}^- + \text{O}_2 + \text{Fe}^{3+}$ ).<sup>30</sup>

Meanwhile, the role of electrostatic charge on the catalytic performance of CL reaction with various catalysts, for example,



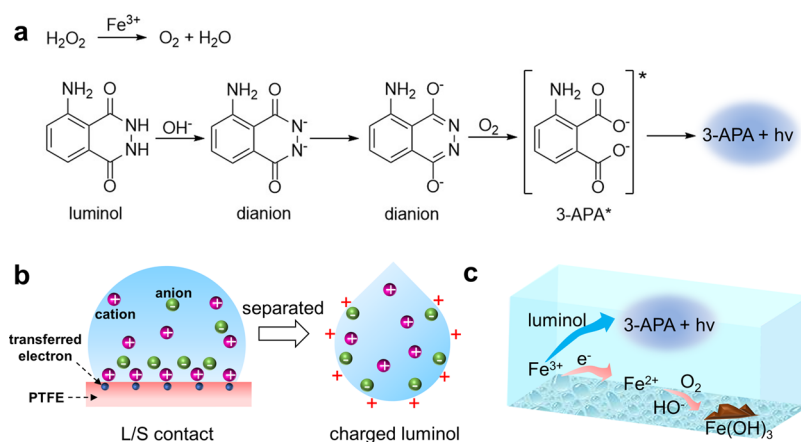


**Figure 4.** Mechanism of electrostatic regulation of CL by electron transfer at the liquid–solid interface. (a) Reaction path to excited-state light-emitting 3-APA\* when luminol dissolved in water contains  $\text{H}_2\text{O}_2$  and  $\text{OH}^-$  and catalysis by  $\text{Fe}^{3+}$ . (b) Schematic depiction of the electron transfer between a liquid droplet and the PTFE interface and thus the ions adsorbed due to the Coulombic attraction. After separation, the positively charged luminol droplet attracts anions at the interface. (c) Schematic depiction of the electrons from the negatively charged luminol droplet competing with luminol for  $\text{Fe}^{3+}$ .

$\text{CuSO}_4$  (3 mM) and  $\text{KMnO}_4$  (3 mM), was also investigated in Figure 2. However, in Figure 2a, we do not see obvious peak shifts. This is probably because when  $\text{CuSO}_4$  is used as a catalyst, the CL emission time is very short compared with  $\text{Fe}^{3+}$  as a catalyst, and thus it is difficult to collect the emission curve at the higher intensity. When the CL intensity is very weak, the emission curve will be frizzy, so the shift is not obvious. In Figure 2b, for the charged luminol– $\text{Cu}^{2+}$  system, stronger CL emission was observed with the addition of the charged luminol droplet into the  $\text{Cu}^{2+}$  solution as compared to the weaker CL emission in the absence of a static charge on the luminol droplet. For the luminol– $\text{MnO}_4^+$  system, although the CL intensity is rather low and the decay time is so fast (Figure 2c,d), a similar trend was also observed: the enhanced CL intensity when the luminol droplet was statically charged. Moreover, the catalytic activity of charged luminol– $\text{Cu}^{2+}$  and luminol– $\text{MnO}_4^+$  systems was also found to increase with the increase of charge on the luminol droplet (Figure 2e), and the reaction time was found to decrease with the increase of charge on the luminol droplet (Figure 2f), which shows the excellent catalytic performance of both statically charged luminol– $\text{Cu}^{2+}$  and luminol– $\text{MnO}_4^+$  systems compared with the absence of charges on the luminol droplet and also indicates that the role of electrostatic charge on the catalytic performance of CL reaction is universal and not limited to a certain kind of catalyst.

However, when the negatively charged luminol droplet is involved in the CL reaction, the story is completely different. Our quantitative data on the inhibitory effect of the negatively charged luminol droplet on the CL reaction in Figure 3 align with this scenario: the more the negative charges on the luminol droplet, weaker CL emission was detected (Figure 3a). The negatively charged luminol droplet was achieved by contacting and separating with different lengths of nylon tubes. When the luminol droplet slides through the nylon tube, the electrons will flow from the nylon surface to the luminol droplet (as nylon has a weak affinity to electrons and therefore it always locates at the top of triboelectric series<sup>31</sup>), with the result being a negatively charged luminol droplet and a positively charged nylon surface. We have tested for CL reaction generated by charged luminol samples bearing a net-negative charge with  $\text{Fe}^{3+}$ . The band center of CL emission

data in Figure 3b, however, seems stable after the statically charged luminol droplet catalyzed by  $\text{Fe}^{3+}$  even when the initial Faraday pail measurement indicates a different net excess of negative charges on the luminol droplets. This is probably because the electric field formed by the small amount of static charge (less than 2 nC) is not enough to influence the energy of emission species. Although the band center is stable for the negatively charged luminol droplet, the relationship between the maximum light intensity and the net charging magnitude of the luminol droplet is clear (Figure 3c,d). Surprisingly, for the negatively charged luminol– $\text{Fe}^{3+}$  system, different from the positively charged luminol– $\text{Fe}^{3+}$  system, weaker CL emissions were observed when the luminol droplets were charged compared to the uncharged luminol droplet (Figure 3c). At the same time, the catalytic activity of the negatively charged luminol– $\text{Fe}^{3+}$  system decreased with the increase of the negative charge on the luminol droplet (Figure 3d). In addition, the time to reach the CL maximum intensity increases with the increase in the amount of negative static charge. All of the above results show that the electrostatic field has two sides to the regulation of the catalytic performance of the CL reaction: positively charged luminol droplet will increase the reaction rate and enhance the CL intensity, while a negatively charged luminol, on the contrary, tends to inhibit the CL.

The light pathway for  $\text{Fe}^{3+}$  catalysis luminol in water has already been well studied in detail.<sup>32</sup> In the presence of a catalyst,  $\text{Fe}^{3+}$ , hydrogen peroxide is first decomposed to form  $\text{O}_2$  and water. Luminol then reacts with  $\text{OH}^-$ , forming a dianion. Then, the  $\text{O}_2$  produced from  $\text{H}_2\text{O}_2$  reacts with the luminol dianion, and an excited light-emitting 3-APA\* is generated (Figure 4a). In the absence of hydrogen peroxide, we recorded no light outputs (Supporting Information, Figure S4). For the enhancement of CL by the positively charged luminol droplet, one first possible explanation is the oxidation of luminol by cationic fragments derived from the dielectric polymer. The material transfer (ionic fragments) could possibly occur between the dielectric polymer and the luminol droplet.<sup>33,34</sup> The cationic fragments should therefore oxidize part of the luminol and thus enhance the CL emission. To test this hypothesis, we carried out contact charging experiments between the luminol droplet and different polymers in

**Supporting Information**, Figure S2. PVC is significantly softer and of higher adhesion than PTFE, and thus there should be a larger material transfer to the luminol droplet from PVC than from PTFE,<sup>7</sup> which would enhance the CL emission more effectively than PTFE if cationic fragments were involved in the catalytic reaction. However, in fact, the data in **Figure S2** show that the catalytic activity of luminol is independent of the type of material but only relates to the amount of static charge. Therefore, the cationic fragment is not a factor for enhancing the CL emission. Electric field is also known to play a crucial role in catalyzing chemical reactions,<sup>4</sup> suggesting that our experiments may be affected by a supply of electrostatic field generated by contact charging between the luminol droplet and PTFE. The electric fields within the ordered solvent environment itself are sufficient to catalyze a chemical reaction.<sup>35</sup> Thus, solvents could be preordered with a field, and then reactions would be allowed to proceed without the external electric field present. In our experiment, the electron transfer occurred between a luminol droplet and the PTFE interface when the luminol droplet slid through the PTFE tube, leading to the negatively charged PTFE surface, and thus the cations were adsorbed on the PTFE due to the Coulombic attraction (**Figure 4b**). After separation, the positively charged luminol droplet attracts anions at the interface and thus creates an ordered solvent environment and promotes the CL emission (**Figure 4b**). We also considered the possibility of anions, such as OH<sup>-</sup>, gathered at the interface of the luminol droplet due to the Coulombic attraction, increasing the concentration of OH<sup>-</sup> at the interface, and when the luminol droplet contacts Fe<sup>3+</sup> solution, the higher concentration of OH<sup>-</sup> at the interface will enhance the CL emission immediately. We observed that increasing the concentration of NaOH (from 0.05 to 0.25 M) will speed up the reaction and enhance the CL emission (**Supporting Information**, Figure S6), suggesting the important role of the concentration of OH<sup>-</sup>. However, for the inhibition of CL by the negatively charged luminol droplet, we remark that it is possible for the electrons from the negatively charged luminol droplet to compete with luminol for Fe<sup>3+</sup>. To support this hypothesis, we note that the concentration of the catalyst, for example, Fe<sup>3+</sup>, influences the decomposition rate of hydrogen peroxide and thus the CL intensity: the lower the concentration of Fe<sup>3+</sup>, the lower the reaction rate and CL intensity (**Supporting Information**, Figure S3). Fe<sup>3+</sup> can be reduced by electrons to Fe<sup>2+</sup> (Fe<sup>3+</sup> + e → Fe<sup>2+</sup>), and in alkaline solutions (in our experiment, the pH of luminol solution is 12), Fe<sup>2+</sup> can be further oxidized to precipitate Fe(OH)<sub>3</sub> (4Fe<sup>2+</sup> + 8OH<sup>-</sup> + O<sub>2</sub> + 2H<sub>2</sub>O → 4Fe(OH)<sub>3</sub>). In this way, the electrons transferred from PTFE to luminol are capable of reducing the amount of catalyst, Fe<sup>3+</sup>, and therefore inhibiting the CL emission (**Figure 4c**).

#### 4. CONCLUSIONS

In this work, we propose a new strategy for electrostatic regulation of CL by electron transfer at the liquid–solid interface. The electron transfer was generated by the luminol droplet sliding on the dielectric polymer surface, and we have first demonstrated a relationship between the sign of the luminol sample (negatively or positively charged) and its effect on the CL reactivity. Our results show that the positively charged luminol droplet will increase the reaction reactivity and enhance the CL intensity, while a negatively charged luminol, on the contrary, tends to inhibit the CL. The transfer

of electrons at the liquid/solid interface appears to be the main cause and more important than the material transfer, ion transfer, and stability of the surface charges in explaining the electrostatic regulation of CL. This work provides a strategy for promoting/inhibiting CL by simply statically charging a reaction solution with a dielectric solid, extends our understanding and control over static electricity with immediate implications in electrostatic catalysis, aids the study of electrostatic forces on chemical reactivity, as well as carries a cautionary message on what to consider when preparing a sample for a chemical reaction.

#### ■ ASSOCIATED CONTENT

##### Supporting Information

The Supporting Information is available free of charge at <https://pubs.acs.org/doi/10.1021/acs.jpcc.1c09402>.

Optical photograph of the light emission system, additional electrostatic electrochemiluminescence spectral data on different plastics and on different concentrations of NaOH, H<sub>2</sub>O<sub>2</sub>, and Fe<sup>3+</sup> (PDF)

#### ■ AUTHOR INFORMATION

##### Corresponding Author

Zhong Lin Wang – Beijing Institute of Nanoenergy and Nanosystems, Chinese Academy of Sciences, Beijing 100083, P. R. China; School of Nanoscience and Technology, University of Chinese Academy of Sciences, Beijing 100049, P. R. China; School of Materials Science and Engineering, Georgia Institute of Technology, Atlanta, Georgia 30332-0245, United States; [orcid.org/0000-0002-5530-0380](https://orcid.org/0000-0002-5530-0380); Email: [zlwang@gatech.edu](mailto:zlwang@gatech.edu)

##### Authors

Jinyang Zhang – Beijing Institute of Nanoenergy and Nanosystems, Chinese Academy of Sciences, Beijing 100083, P. R. China; School of Nanoscience and Technology, University of Chinese Academy of Sciences, Beijing 100049, P. R. China

Shiquan Lin – Beijing Institute of Nanoenergy and Nanosystems, Chinese Academy of Sciences, Beijing 100083, P. R. China; School of Nanoscience and Technology, University of Chinese Academy of Sciences, Beijing 100049, P. R. China

Complete contact information is available at: <https://pubs.acs.org/10.1021/acs.jpcc.1c09402>

##### Author Contributions

<sup>||</sup>J.Z. and S.L. are contributed equally to this work.

##### Notes

The authors declare no competing financial interest.

#### ■ ACKNOWLEDGMENTS

J.Z. and S.L. contributed equally to this work. Research was supported by the National Key R&D Project from Minister of Science and Technology (2016YFA0202704) and the National Natural Science Foundation of China (grant nos. 52005044 and 22102010).

#### ■ REFERENCES

- (1) Zhang, L.; Vogel, Y. B.; Noble, B. B.; Gonçalves, V. R.; Darwish, N.; Brun, A. L.; Gooding, J. J.; Wallace, G. G.; Coote, M. L.; Ciampi, S. TEMPO Monolayers on Si (100) Electrodes: Electrostatic Effects

- by The Electrolyte and Semiconductor Space-Charge on The Electroactivity of A Persistent Radical. *J. Am. Chem. Soc.* **2016**, *138*, 9611–9619.
- (2) Warshel, A.; Sharma, P. K.; Kato, M.; Xiang, Y.; Liu, H.; Olsson, M. H. M. Electrostatic basis for enzyme catalysis. *Chem. Rev.* **2006**, *106*, 3210–3235.
- (3) Fried, S. D.; Boxer, S. G. Electric fields and enzyme catalysis. *Annu. Rev. Biochem.* **2017**, *86*, 387–415.
- (4) Ciampi, S.; Diez-Perez, I.; Coote, M. L.; Darwish, N. Experimentally Harnessing Electric Fields in Chemical Transformations. *Effects of Electric Fields on Structure and Reactivity*; Royal Society of Chemistry, 2021; Chapter 3, pp 71–118.
- (5) Marcus, R. A. On the theory of oxidation-reduction reactions involving electron transfer. I. *J. Chem. Phys.* **1956**, *24*, 966–978.
- (6) Aragonès, A. C.; Haworth, N. L.; Darwish, N.; Ciampi, S.; Bloomfield, N. J.; Wallace, G. G.; Diez-Perez, I.; Coote, M. L. Electrostatic Catalysis of a Diels–Alder Reaction. *Nature* **2016**, *531*, 88–91.
- (7) Zhang, J.; Ferrie, S.; Zhang, S.; Vogel, Y. B.; Peiris, C. R.; Darwish, N.; Ciampi, S. Single-Electrode Electrochemistry: Chemically Engineering Surface Adhesion and Hardness to Maximize Redox Work Extracted from Tribocharged Silicon. *ACS Appl. Nano Mater.* **2019**, *2*, 7230–7236.
- (8) Zhang, J.; Coote, M. L.; Ciampi, S. Electrostatics and Electrochemistry: Mechanism and Scope of Charge-Transfer Reactions on the Surface of Tribocharged Insulators. *J. Am. Chem. Soc.* **2021**, *143*, 3019–3032.
- (9) Zhang, J.; Rogers, F. J. M.; Darwish, N.; Gonçalves, V. R.; Vogel, Y. B.; Wang, F.; Gooding, J. J.; Peiris, M. C. R.; Jia, G.; Veder, J.-P.; Coote, M. L.; Ciampi, S. Electrochemistry on Tribocharged Polymers Is Governed by the Stability of Surface Charges Rather than Charging Magnitude. *J. Am. Chem. Soc.* **2019**, *141*, 5863.
- (10) Liu, C.-y.; Bard, A. J. Electrons on Dielectrics and Contact Electrification. *Chem. Phys. Lett.* **2009**, *480*, 145–156.
- (11) Zhang, J.; Darwish, N.; Coote, M. L.; Ciampi, S. Static Electrification of Plastics under Friction: The Position of Engineering-Grade Polyethylene Terephthalate in the Triboelectric Series. *Adv. Eng. Mater.* **2019**, *22*, 1901201.
- (12) Li, X.; Zhang, L.; Feng, Y.; Zhang, X.; Wang, D.; Zhou, F. Solid–Liquid Triboelectrification Control and Antistatic Materials Design Based on Interface Wettability Control. *Adv. Funct. Mater.* **2019**, *29*, 1903587.
- (13) Lin, S.; Xu, L.; Wang, A. C.; Wang, Z. L. Quantifying Electron-Transfer in Liquid-Solid Contact Electrification and the Formation of Electric Double-Layer. *Nat. Commun.* **2020**, *11*, 1–8.
- (14) Lin, S.; Zheng, M.; Luo, J.; Wang, Z. L. Effects of Surface Functional Groups on Electron Transfer at Liquid–Solid Interfacial Contact Electrification. *ACS Nano* **2020**, *14*, 10733–10741.
- (15) Tang, W.; Chen, B. D.; Wang, Z. L. Recent Progress in Power Generation from Water/Liquid Droplet Interaction with Solid Surfaces. *Adv. Funct. Mater.* **2019**, *29*, 1901069.
- (16) Xu, L.; Pang, Y.; Zhang, C.; Jiang, T.; Chen, X.; Luo, J.; Tang, W.; Cao, X.; Wang, Z. L. Integrated Triboelectric Nanogenerator Array Based on Air-Driven Membrane Structures for Water Wave Energy Harvesting. *Nano Energy* **2017**, *31*, 351–358.
- (17) Yang, L.; Wang, Y.; Guo, Y.; Zhang, W.; Zhao, Z. Robust Working Mechanism of Water Droplet-Driven Triboelectric Nanogenerator: Triboelectric Output versus Dynamic Motion of Water Droplet. *Adv. Mater. Interfaces* **2019**, *6*, 1901547.
- (18) Zhan, F.; Wang, A. C.; Xu, L.; Lin, S.; Shao, J.; Chen, X.; Wang, Z. L. Electron Transfer as a Liquid Droplet Contacting a Polymer Surface. *ACS Nano* **2020**, *14*, 17565–17573.
- (19) Lim, K. H.; Sun, Y.; Lim, W. C.; Soh, S. Charging Organic Liquids by Static Charge. *J. Am. Chem. Soc.* **2020**, *142*, 21004.
- (20) Zhang, J.; Lin, S.; Zheng, M.; Wang, Z. L. Triboelectric Nanogenerator as a Probe for Measuring the Charge Transfer between Liquid and Solid Surfaces. *ACS Nano* **2021**, *15*, 14830–14837.
- (21) Zhang, J.; Ciampi, S. Shape and Charge: Faraday’s Ice Pail Experiment Revisited. *ACS Cent. Sci.* **2020**, *6*, 611–612.
- (22) Pandey, R. K.; Ao, C. K.; Lim, W.; Sun, Y.; Di, X.; Nakanishi, H.; Soh, S. The Relationship between Static Charge and Shape. *ACS Cent. Sci.* **2020**, *6*, 704–714.
- (23) Nie, J.; Ren, Z.; Xu, L.; Lin, S.; Zhan, F.; Chen, X.; Wang, Z. L. Probing Contact-Electrification-Induced Electron and Ion Transfers at a Liquid–Solid Interface. *Adv. Mater.* **2020**, *32*, 1905696.
- (24) Lin, S.; Chen, X.; Wang, Z. L. Contact Electrification at the Liquid–Solid Interface. *Chem. Rev.* **2022**, *122*, 5209.
- (25) White, E. H.; Bursley, M. M. Chemiluminescence of luminol and related hydrazides: the light emission step. *J. Am. Chem. Soc.* **1964**, *86*, 941–942.
- (26) Giussani, A.; Farahani, P.; Martínez-Muñoz, D.; Lundberg, M.; Lindh, R.; Roca-Sanjuán, D. Molecular basis of the chemiluminescence mechanism of luminol. *Chem.—Eur. J.* **2019**, *25*, 5202–5213.
- (27) Chen, A.; Zhang, C.; Zhu, G.; Wang, Z. L. Polymer Materials for High-Performance Triboelectric Nanogenerators. *Adv. Sci.* **2020**, *7*, 2000186.
- (28) Chen, X.; Xing, L.-L.; Tang, Y.-H.; Zhang, G.-B. Luminol–K3Fe (CN) 6 chemiluminescence system for the determination of glipizide. *J. Pharm. Anal.* **2013**, *3*, 127–131.
- (29) Shevlin, P. B.; Neufeld, H. A. Mechanism of the ferricyanide-catalyzed chemiluminescence of luminol. *J. Org. Chem.* **1970**, *35*, 2178–2182.
- (30) Kremer, M. L.; Stein, G. Kinetics of the Fe<sup>3+</sup> ion–H<sub>2</sub>O<sub>2</sub> reaction: Steady-state and terminal-state analysis. *Int. J. Chem. Kinet.* **1977**, *9*, 179–184.
- (31) Zhang, J.; Ciampi, S. The Position of Solid Carbon Dioxide in The Triboelectric Series. *Aust. J. Chem.* **2019**, *72*, 633–636.
- (32) Bi, S.; Zhou, H.; Zhang, S. Bio-bar-code functionalized magnetic nanoparticle label for ultrasensitive flow injection chemiluminescence detection of DNA hybridization. *Chem. Commun.* **2009**, 5567–5569.
- (33) Baytekin, H. T.; Baytekin, B.; Incorvati, J. T.; Grzybowski, B. A. Material Transfer and Polarity Reversal in Contact Charging. *Angew. Chem., Int. Ed.* **2012**, *51*, 4843–4847.
- (34) Zhang, J.; Su, C.; Rogers, F. J. M.; Darwish, N.; Coote, M. L.; Ciampi, S. Irreproducibility in the Triboelectric Charging of Insulators: Evidence of a Non-Monotonic Charge versus Contact Time Relationship. *Phys. Chem. Chem. Phys.* **2020**, *22*, 11671–11677.
- (35) Xu, L.; Izgorodina, E. I.; Coote, M. L. Ordered solvents and ionic liquids can be harnessed for electrostatic catalysis. *J. Am. Chem. Soc.* **2020**, *142*, 12826–12833.